BUTTERWORTH HEINEMANN

Polymer Vol. 36 No. 6, pp. 1167–1178, 1995

0032-3861/95/$10.00+0.00

Processing of intractable polymers using reactive solvents: 2. Poly(2,6-dimethyl-1,4-phenylene ether) as a matrix material for high performance composites

R. W. Venderbosch, H. E. H. Meijer and P. J. Lemstra*

Centre for Polymers and Composites, Eindhoven University of Technology, PO Box 513, Den Dolech 2, 5600 MB Eindhoven, The Netherlands
(Received 23 March 1994; revised 31 August 1994)

The application of poly(2,6-dimethyl-1,4-phenylene ether) (PPE) as a matrix material for continuous carbon fibre reinforced composites has been studied. Owing to the intractable nature of PPE, melt impregnation is not feasible and therefore a solution impregnation route was explored using epoxy resin as a reactive solvent. The introduction of epoxy resin results in enhanced flow and reduced processing temperatures, enabling the processing of PPE and the preparation of high quality composites. Upon curing the homogeneous epoxy/PPE solutions, phase separation is initiated and the epoxy resin is converted into a dispersed phase. In composites, the epoxy resin preferentially accumulates at the polar fibre surfaces present, resulting in an epoxy layer around the fibre and consequently a high level of interfacial adhesion. For high fibre volume fractions (>50%), a morphology of epoxy-coated fibres in a pure PPE matrix is obtained. Owing to this unique morphology, the resulting thermoplastic composite materials reveal outstanding mechanical properties with a pronounced synergy in mode-II interlaminar toughness and impact performance.

(Keywords: intractable polymers; thermoplastic composites; epoxy resin)

INTRODUCTION

Continuous carbon fibre reinforced composites are increasingly used as structural materials, mainly owing to their high stiffness per unit weight as compared with metals. It is, however, well recognized that the optimal performance in terms of weight-saving efficiency is often limited by their low damage tolerance[1,2], especially in the most commonly encountered case of brittle thermosetting matrices. A considerable increase in damage tolerance can be achieved by using tough, high performance plastics as matrix material[3], such as poly(ether ether ketone)[4] (PEEK).

Another interesting polymer for the production of tough, thermoplastic composites is poly(2,6-dimethyl-1,4-phenylene ether) (PPE). PPE is a relatively low cost amorphous thermoplastic with a high glass transition temperature (T_g) of approximately 220°C and excellent mechanical properties, e.g. in terms of toughness. However, as a result of its limited thermal and oxidative stability, PPE cannot be melt processed. The high temperatures required for melt processing (300–350°C) will yield severe degradation, and therefore PPE is usually classified as intractable. In practice, PPE is only applied in blends[5], notably the miscible system PPE/polystyrene, which exhibits a lower T_g and subsequently allows for considerably lower processing temperatures. The decrease in T_g of the final product is the penalty for introducing processability to PPE.

Since melt impregnation routes apparently are not feasible, a solution impregnation route has to be considered to introduce PPE as a matrix material in composites. Conventional solution impregnation techniques that use, for instance, methylene chloride as a solvent will, however, introduce additional problems related to the complete elimination of residual solvent from the composite material. Residual traces of solvent in the material result in a reduction in the mechanical properties, especially at elevated temperatures. Other problems involve voids in the composite structure and a less satisfactory interface control, resulting in a reduction of the overall composite performance. For instance, as shown by Cogswell *et al.*[6] for poly(ether sulfone)-based composites, during extraction the solvent tends to accumulate and migrate along the fibre surface, causing detachment of the resin from the interface.

A challenging solution to these problems can be found in the use of reactive solvents. In our earlier paper[7], a reactive processing technique was explored for PPE, based on the use of standard bisphenol-A epoxy resin as a reactive solvent. In contrast to the literature[8–24] on blends of epoxy resins with engineering plastics which mainly aims at toughened thermosets or hybrids of thermosets and thermoplastics, in this processing

*To whom correspondence should be addressed

technique the epoxy resin is only introduced in order to tune the processability of the thermoplastic. In accordance with conventional solvent techniques, this results in enhanced flow and reduced processing temperatures. Instead of the complicated solvent recovery step, which is the major disadvantage of every conventional solvent technique, the homogeneous solution is cured after processing. During curing the epoxy resin is converted into a non-solvent and phase separation is initiated. For PPE contents exceeding 15 wt%, phase separation is accompanied by phase inversion. Consequently, PPE is regained and the solvent is converted into a dispersed phase. As a result of the moderate processing temperatures applied, extensive degradation of PPE is prevented. Moreover, at curing temperatures close to the glass transition temperature of PPE, the phase separation process is virtually complete[7], yielding materials with a T_g of 220°C for the continuous PPE phase. Consequently, in contrast to PPE/polystyrene blends, the enhanced processability is not obtained at the expense of the T_g.

In this paper, the above-described reactive processing technique is studied as a route to introduce PPE into high performance composite structures. Firstly, the characteristics of the blends of PPE and epoxy resin are discussed briefly. Secondly, the influence of the presence of fibres on the blend morphology which results from phase separation is studied. Finally, the morphologies and mechanical properties of carbon fibre reinforced composites are presented.

EXPERIMENTAL

Matrix materials

Poly(2,6-dimethyl-1,4-phenylene ether) (PPE 803) with a weight-average molecular weight of 32 kg mol^{-1} ($M_w/M_n = 2.3$) was supplied by General Electric Plastics. A standard diglycidyl ether of bisphenol-A (DGEBA, Epikote 828EL) was used as a reactive solvent and was supplied by Shell. Both the epoxy resin and the epoxy/PPE blends were cured using 4,4′-methylenebis(3-chloro-2,6-diethylaniline) (M-CDEA) supplied by Lonza or diethyltoluenediamine (Ethacure 100) supplied by Ethyl Corporation. The M-CDEA curing agent was of particular importance in this investigation owing to its relatively low toxicity, volatility and reactivity, yielding materials which were easy to handle on a laboratory scale.

Solutions of PPE in epoxy resin were prepared in a Brabender Plasticorder kneader. At a kneading temperature of 175°C a kneading time of ~1 h was required to obtain transparent homogeneous solutions. After addition of the curing agent, mixing was continued for <5 min in the case of Ethacure 100 and 10–15 min in the case of M-CDEA.

From these compounds, thin films required for the composite preparation were compression moulded in a hot press in between aluminium foils (50 bar, 175°C, 5 min). The area where the polymer could flow during pressing was restricted by using two metal strips as long as the hot plates of the press and with a thickness of 0.2 mm. As soon as the molten material started to flow out of the 'mould', the film was quenched in a water-cooled press. This technique enabled us to prepare void-free films with a high reproducibility, since the film thickness (with an accuracy of ±0.01 mm) was controlled by the amount of polymer. Fortunately, the uncured polymer did not adhere to the aluminium foils and no release agents were required.

Alternatively, plates required to determine the mechanical properties of the epoxy/PPE systems were moulded and cured by using an oblong-shaped open mould (stainless steel) in between aluminium foils. Both the mould and aluminium foils had to be treated with release agent (Freekote 44, Hysol Corporation) because the compound revealed excellent adhesion to metals after curing. In general, a curing cycle of 2 h at 225°C was applied followed by a post-cure of 4 h at 200°C in an inert atmosphere.

Specimens of pure PPE and epoxy resin cured with M-CDEA were prepared by using conventional compression-moulding and casting techniques, respectively, under the same conditions as were used during the composite preparation.

Composite preparation

Chopped carbon fibre reinforced composites (17 vol% fibres of 5 mm length) were prepared as model materials. The E-glass fibre (standard silane sizing) were supplied by PPG Industries and carbon fibres (Grafil XA-S/3K and surface-treated and untreated Apollo IM-43-750/3K) were supplied by Courtaulds. The chopped fibres were dispersed in the homogeneous epoxy/PPE solution using a Brabender kneader (175°C, 44 wt% PPE, 25 parts per hundred parts of resin by weight (phr) Ethacure 100). The composite compound was immediately moulded and cured in a hot press for 2 h at 225°C and post-cured for 4 h at 200°C.

Continuous carbon fibre reinforced composites were prepared using plain weave fabrics (T300 fibre, CD168, 168 g m^{-2}) supplied by Ten Cate. Composites based on the epoxy/PPE system (40 and 60 wt% PPE, 55 phr M-CDEA) were prepared by film stacking (nominal film thickness 0.2 mm). Owing to the use of relatively thick films, one epoxy/PPE film was incorporated for every two fabrics. The laminates were consolidated in a hot press for 2 h at a temperature of 225°C and at a relatively low pressure of 5 bar in a Teflon vacuum bag. A post-cure for 4 h at 200°C was applied. Besides the laminates based on the epoxy/PPE blends, reference materials were prepared based on pure epoxy resin (55 phr M-CDEA) and on pure PPE. The laminates were prepared by hand lay-up of preimpregnated fabrics. The PPE matrix prepregs were prepared by solution impregnation using chloroform ($CHCl_3$) as a solvent. After drying under ambient conditions for at least 24 h, the chloroform was removed under vacuum at a temperature of 100°C over 4 h. The neat PPE laminates were consolidated at a temperature of 300°C for <8 min at a pressure of 150 bar. The epoxy matrix prepregs were, after impregnation, pre-cured for 12 h at 100°C. The epoxy laminates were consolidated under the same conditions as applied for the epoxy/PPE laminates except for the temperature, which was 175°C. All the composites prepared had a nominal fibre volume fraction of 50–55%. Specimens were cut from the composite plates with a diamond cutting wheel.

Mechanical testing

Unless indicated otherwise, all the mechanical tests were performed at room temperature using a Frank

tensile tester (81565 IV), and an average was taken from at least five specimens of each composition.

The tensile moduli and strengths of the neat matrix materials were determined from edge-polished specimens with dimensions according to ASTM D 638 (2 mm thick, 13 mm wide in the narrow section, 180 mm long). The experiments were performed using an extensometer ($l_0 = 50$ mm) at a strain rate of $10^{-3}\,s^{-1}$. The mode-I fracture toughnesses[25] of the matrix materials were determined using the three-point bend specimen geometry. In order to ensure plane strain conditions, a central V-shaped notch was machined and additionally sharpened with a fresh razor blade (total depth 5 mm). The specimens ($4 \times 10 \times 50\,mm^3$) were tested using a span to depth ratio of 4 and a crosshead speed of $10\,mm\,min^{-1}$.

The moduli and strengths of the carbon fabric laminates were determined using a three-point bend test set-up according to ASTM D 790. The samples ($1.8 \times 15 \times 90\,mm^3$) with a lay-up sequence of $[(0,90)]_{10}$ (denoting 10 plies of fabrics stacked in a 0°/90° lay-up) were tested using a span to depth ratio of 30 and a crosshead speed of $10\,mm\,min^{-1}$.

The mode-I and mode-II interlaminar fracture toughnesses[26] of the carbon fabric laminates were determined using the double-cantilever beam (DCB) geometry and the end-notched flexure (ENF) specimen geometry, respectively. To initiate delamination an aluminium foil (35 mm long, 0.01 mm thick) coated wih release agent (Freekote 44, Hysol Corporation) was placed at the laminate mid-thickness prior to moulding. The mode-I DCB specimens ($[(0,90)]_{20}$ lay-up, 3.6 mm thick, 20 mm wide) were not precracked before testing and were loaded at a crosshead speed of $0.5\,mm\,min^{-1}$. This test set-up facilitates the measurement of the critical strain energy release rate G_{Ic} as a function of crack length (the resistance (R) curve). The propagation value for G_{Ic} is the average value calculated in the range of ratios of displacements to crack lengths of 0.2–0.4. The data were analysed according to the corrected beam theory[26]. The mode-II specimens ($[(0,90)]_{20}$ lay-up, 3.6 mm thick, 20 mm wide) were loaded at a crosshead speed of $1\,mm\,min^{-1}$ in three-point bending using a ratio of crack length to half-span of 0.5. By using this test set-up an initiation value for G_{IIc} was determined. The specimens were precracked in shear in order to avoid effects from the aluminium starter defect. The length of this precrack was measured using an Olympus optical microscope (BH2-MA-2). After repositioning of the sample, an initiation value for G_{IIc} was determined using an increase in the initial compliance of 5% as the criterion for crack initiation. However, for the brittle epoxy matrix composites the maximum load was taken as the criterion for crack initiation. The data were analysed according to the direct beam theory[26].

The impact performance of the carbon fabric laminates was studied utilizing a falling weight impact tester (by courtesy of the Catholic University of Leuven, Belgium). Impacts were effected by dropping a hemispherical dart (16 mm diameter) onto composite specimens ($[(0,90)]_{10}$ lay-up, $1.8 \times 90 \times 90\,mm^3$) which were clamped between two plates with a square cut-out of $80 \times 80\,mm^2$. The impact energy was controlled by varying the initial height and weight of the dart. The incident energy was varied from 3 to 21 J. Both force *versus* time and impact velocity just before impact were recorded and stored in a digital storage oscilloscope. Subsequent processing of the data resulted in the complete energy history during impact and the energy absorbed by the composite. The internal damage, such as delaminations, was analysed using an ultrasonic C-scan (Physical Acoustics Corporation). The residual strengths of the impacted specimens were measured using a three-point bend test set-up with a span to depth ratio of 40 and a crosshead speed of $10\,mm\,min^{-1}$. The results were normalized to the strength of the non-damaged sample. This series of tests was performed on three specimens for each composition and impact energy, with the exception of the highest impact energies of 18 and 21 J for the epoxy/PPE specimens with 40 wt% PPE and 60 wt% PPE, respectively, which were single-point measurements.

The impact performance of the composites was additionally studied using a compression after impact test (CAI). Quasi-isotropic specimens (150 mm long, 100 mm wide, 5 mm thick) consisting of 27 plies of carbon fabric in a 0°/45° lay-up, i.e. $[((0,90)/(-45,+45))_{13}/(0,90)]$, were impacted and tested according to the specifications of the BOEING compression after impact test (BSS 7260, $6.7\,J\,mm^{-1}$, impact support with a $75 \times 125\,mm^2$ cut-out), The compressive strengths (CSAI) of the impacted samples were measured using an antibuckling guide on a Zwick 1484 tensile machine at a crosshead speed of $0.5\,mm\,min^{-1}$. Owing to the exceptionally large geometry of the plates, for each composition only one plate could be tested.

Morphologies

The morphologies of the matrix materials and the composites were studied from gold/palladium-coated fracture surfaces using a Cambridge Stereoscan 200 scanning electron microscope. No additional staining techniques were applied.

RESULTS AND DISCUSSION

Morphology and properties of the epoxy/PPE system

At elevated temperatures (>150°C) PPE can be dissolved in epoxy resin (including the curing agent) to give medium viscosity compounds which can be relatively easily processed at temperatures between 175 and 225°C[7]. Upon curing of the homogeneous solutions, phase separation will inevitably occur: the increase in molecular weight of the epoxy resin and the resulting change in the polarity of the system due to the conversion of the reactive groups yield a drastic decrease in miscibility of the system. In *Figure 1* scanning electron microscopy (SEM) micrographs are presented of fracture surfaces of the cured epoxy/PPE blends used as matrix material. In both blends (PPE contents of 40 and 60 wt%) phase separation and phase inversion are observed, i.e. a morphology of epoxy spheres dispersed in a continuous PPE matrix. Consequently, after curing PPE is regained and the epoxy resin solvent is converted into a dispersed phase.

In agreement with the results reported in our previous paper[7] for epoxy/PPE blends cured with Ethacure 100, in *Figure 1* a significant decrease in the diameter of the dispersed epoxy spheres is observed with increasing PPE content. This effect is the result of the increase in viscosity of the solutions. In the case of a solution with a higher viscosity, the coarsening process of the spinodal demixed

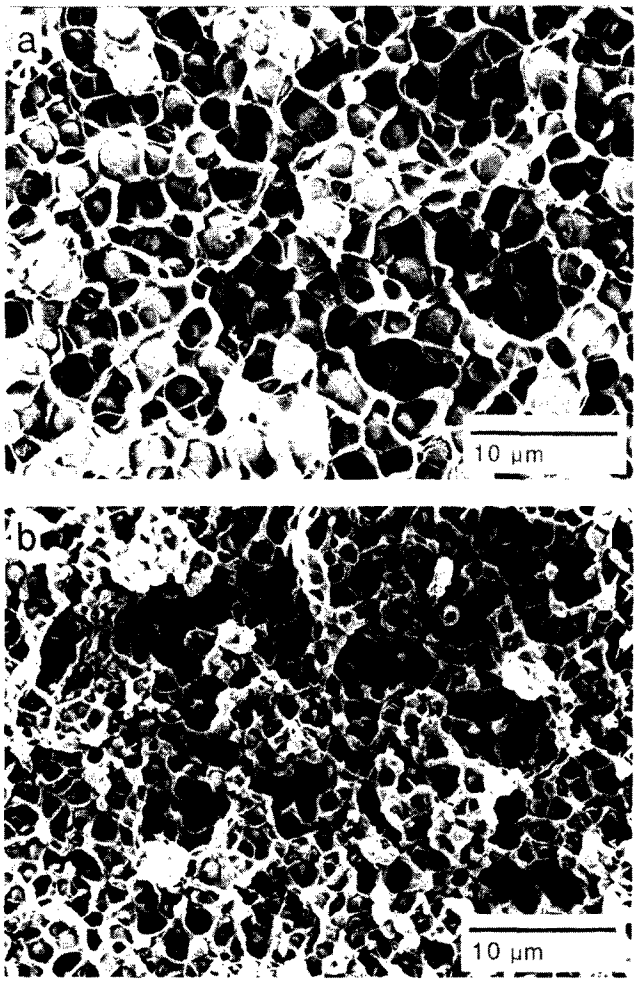

Figure 1 SEM micrographs of fracture surfaces of cured blends (T_{cure} = 225°C, 55 phr M-CDEA) of PPE (32 kg mol^{-1}) and epoxy resin: (a) 40 wt% PPE; (b) 60 wt% PPE

Table 1 Mechanical properties of the epoxy, PPE and epoxy/PPE systems (the sample standard deviations are given in parentheses)

	E (GPa)	σ (MPa)	G_{Ic} (kJ m^{-2})
Epoxy	2.4 (0.07)	67.1[a] (7.03)	0.23 (0.04)
Blend (40 wt% PPE)	2.3 (0.06)	71.8[b] (0.87)	3.7 (0.12)
Blend (60 wt% PPE)	2.3 (0.21)	75.0[b] (3.00)	4.3 (0.19)
PPE	2.4 (0.08)	70.1[b] (0.64)	5.9 (0.20)

[a]Stress at break
[b]Yield stress

solution will be hindered more and will result in a finer morphology.

The mechanical properties of the polymer blends and of both pure constituents are presented in *Table 1*. In general, the mechanical and thermal properties are dominated by PPE, and materials that combine a high T_g with excellent mode-I fracture toughness are obtained. The blends exhibit a high tensile strength, which is indicative of a sufficient level of adhesion between both phases. An interesting feature is that the Young's modulus of PPE is approximately equal to the modulus of the cured epoxy system. As a result, at moderate strain levels only minor stress concentrations are induced in the material despite its pronounced heterogeneity. However, at higher stress levels which initiate yielding of the PPE matrix, the relatively rigid epoxy spheres restrain extensive macroscopic yielding. Tensile experiments reveal initiation of a small yielding zone or neck as soon as the yield stress is reached, rapidly followed by catastrophic failure. Despite the high level of localized plastic deformation in the yield zone (> 25%), this results macroscopically in a rather low elongation to failure of less than 10%. Additionally, owing to the presence of the glassy, brittle epoxy spheres, the toughness of the blend is decreased in comparison with pure PPE. In accordance with the results presented in our previous paper[7], the mode-I fracture toughness of the epoxy/PPE blend decreases with increasing epoxy content.

Composite morphology

Upon incorporating fibres into the epoxy/PPE system, not only is a reinforcement added but additionally a large amount of interface is introduced. It has been shown in the literature[4] that the matrix characteristics can be influenced by the presence of such a fibre interface. For instance, in carbon fibre reinforced semicrystalline thermoplastics the fibre surface may influence the nucleation and growth of spherulites within the matrix. Therefore, the influence of the incorporation of fibres on the final blend morphology after phase separation was studied first. This study was performed using composites reinforced with short fibres.

In *Figures 2a* and *2b* the morphologies of an epoxy/PPE blend (containing 44 wt% PPE) in the vicinity of a carbon fibre and glass fibre, respectively, are shown. The SEM micrographs of the fracture surfaces reveal a remarkable influence of the presence of fibres on the final morphology of the blend. Epoxy resin preferentially accumulates at the fibre surface, resulting in an epoxy 'interlayer' around the fibre. It is not clear if this morphology is the result of the fibre surface acting as a nucleus for phase separation or is caused by a migration or coalescence mechanism during the coarsening process of the demixed blend after phase separation. However, it is likely that the polarity of the fibre surface plays an important role: as a consequence of the higher polarity of the epoxy resin compared with PPE, the epoxy resin will prefer to be located at the polar interface.

In order to investigate this hypothesis, the experiment was repeated using surface-treated and untreated carbon fibres. In general, commercially produced carbon fibres are surface treated in order to facilitate wetting and to improve adhesion[27–29]. The oxidative surface modification increases the amount of chemically bound oxygen and consequently the fibre surface polarity. In *Figures 2c* and *2d* the influence of fibre treatment on the matrix morphology is illustrated. Besides a pronounced influence on fibre/matrix adhesion, it is observed that an increase in surface treatment results in a significant increase in the 'interlayer' thickness. Around the treated carbon fibre a bulky epoxy layer is present, while around the untreated fibre such an epoxy layer cannot be distinguished. This clearly illustrates that the polarity of the fibre surface is the main driving force for the accumulation of epoxy resin at the fibre/matrix interface. Moreover, this will occur at every polar interface (for instance, also at metal substrates) and is likely to provide a high level of interfacial adhesion.

The epoxy/PPE system was used as a matrix material in continuous carbon fibre reinforced composites. Using

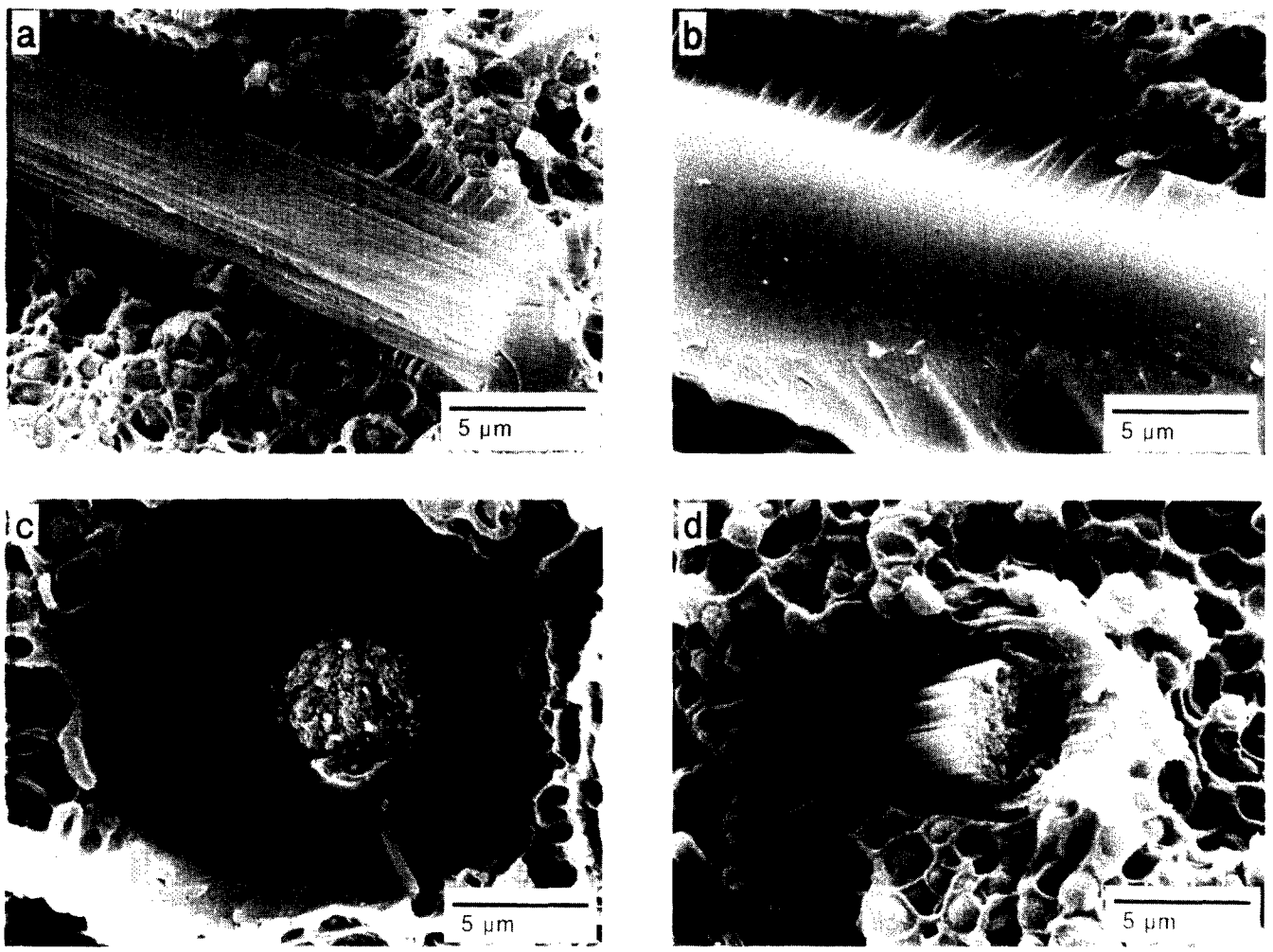

Figure 2 SEM micrographs of fracture surfaces of short fibre reinforced composites (17 vol% fibres) based on epoxy/PPE blends (44 wt% PPE, 25 phr Ethacure 100): (a) Grafil XA-S carbon fibre; (b) E-glass fibre; (c) treated Apollo IM carbon fibre; (d) untreated Apollo IM carbon fibre

the epoxy resin as a reactive solvent, the viscosity of PPE at an impregnation temperature of 225°C could be reduced to approximately 50 and 750 Pa s for 40 and 60 wt% PPE, respectively. These medium viscosity compounds can be easily used in a film-stacking technique to prepare carbon fabric reinforced composites with a fibre volume fraction of 50% under low pressure conditions. In *Figure 3* a polished cross-section of such a composite is shown. This optical micrograph demonstrates that the reactive processing technique enables the preparation of PPE-based composites that exhibit a low void content and an excellent degree of impregnation.

A more detailed study of the carbon fabric laminates revealed a significant influence of the fibre volume fraction on the final composite morphology. In matrix-rich areas the morphology corresponds to the one found earlier for the short fibre reinforced composites, i.e. epoxy-coated fibres in a continuous PPE-rich matrix containing dispersed epoxy particles. In contrast, in fibre-rich areas (see *Figure 4*) no dispersed epoxy particles can be distinguished in the PPE matrix. Consequently, the majority of the epoxy resin migrates to the fibre surface, resulting in a unique morphology of epoxy-coated fibres in a nearly pure PPE matrix.

Based on the morphological observations, it is concluded that the epoxy resin is not only effective as a solvent during processing, enabling processing of PPE and the incorporation of PPE into composite structures, but provides additionally a structural part (i.e. the interphase) of the final composite material after curing. Moreover, this implies that the morphology and mechanical properties are different for the pure polymer

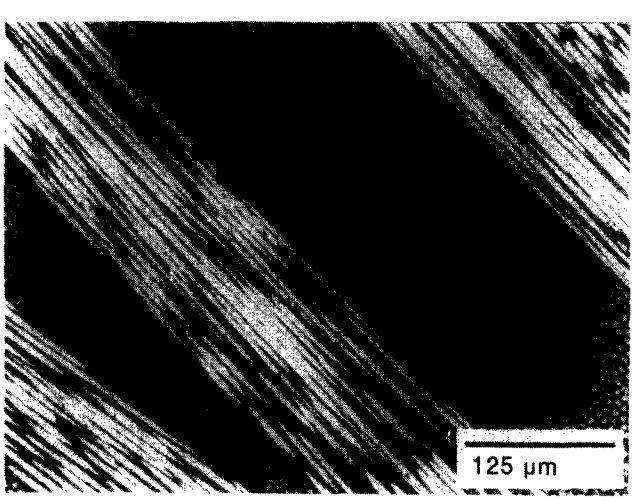

Figure 3 Optical micrograph of a polished cross-section of an epoxy/PPE-based (60 wt% PPE, 55 phr M-CDEA) carbon fabric reinforced composite (50 vol% fibres)

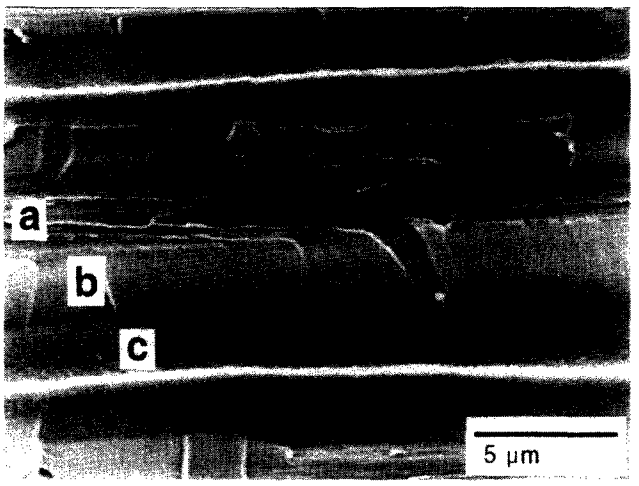

Figure 4 SEM micrograph of a fracture surface in a fibre-rich area of an epoxy/PPE-based (60 wt% PPE, 55 phr M-CDEA) carbon fabric reinforced composite (50 vol% fibres): (a) fibre (imprint); (b) epoxy layer; (c) PPE matrix

Table 2 Flexural properties of carbon fabric laminates (50 vol% fibres) based on epoxy/PPE blends and the epoxy system (the sample standard deviations are given in parentheses)

	E (GPa)	σ (MPa)
Epoxy	43.9 (2.17)	676 (49.1)
Blend (40 wt% PPE)	43.0 (2.50)	715 (47.1)
Blend (60 wt% PPE)	44.8 (2.64)	740 (50.4)

blend and the same material used as a matrix material in composite structures.

Flexural performance

Some flexural properties of the fabric laminates are presented in *Table 2*. Comparing the results found for the epoxy/PPE laminates with those for the pure epoxy resin laminate, it is concluded that the reactive processing route yields high quality composites with good impregnation and a high level of interfacial adhesion.

Interlaminar mode-I and mode-II fracture toughnesses

The main reason for introducing PPE into continuous carbon fibre reinforced composites is its high ductility or toughness. For this reason, the mode-I and mode-II interlaminar fracture toughnesses of the laminates were studied.

In *Figure 5a* the critical strain energy release rate values G_{Ic} obtained for the composites based on the neat constituents and the blends are presented. As can be derived from *Figure 5a*, the application of epoxy/PPE blends as matrix materials results in composites with relatively high G_{Ic} values. The correlation between composite mode-I fracture toughness and PPE content (or matrix ductility; see *Table 1*) agrees well with the results reported in the literature. As shown by Bradley[30], no linear correlation exists between matrix (G_{Ic}^{M}) and composite (G_{Ic}^{C}) mode-I fracture toughnesses. Generally, for brittle matrix materials ($G_{Ic} < 0.4$ kJ m^{-2}, e.g. epoxy resin) a delamination fracture toughness is observed which is higher than the fracture toughness of the pure resin. This is explained by the increase in fracture surface as a result of the curved crack path imposed by the presence of fibres. For ductile matrix materials, on the other hand, the neat resin fracture toughness is only partly translated into the composite fracture toughness and an 'upper limit' for G_{Ic}^{C} is found of approximately 2 kJ m^{-2}. The rather disappointingly low G_{Ic}^{C} values are related to the high volume fraction of high modulus fibres which prevent the development of a large plastic zone at the crack tip. For the epoxy/PPE-based composites this upper limit is reached at low PPE contents. A positive

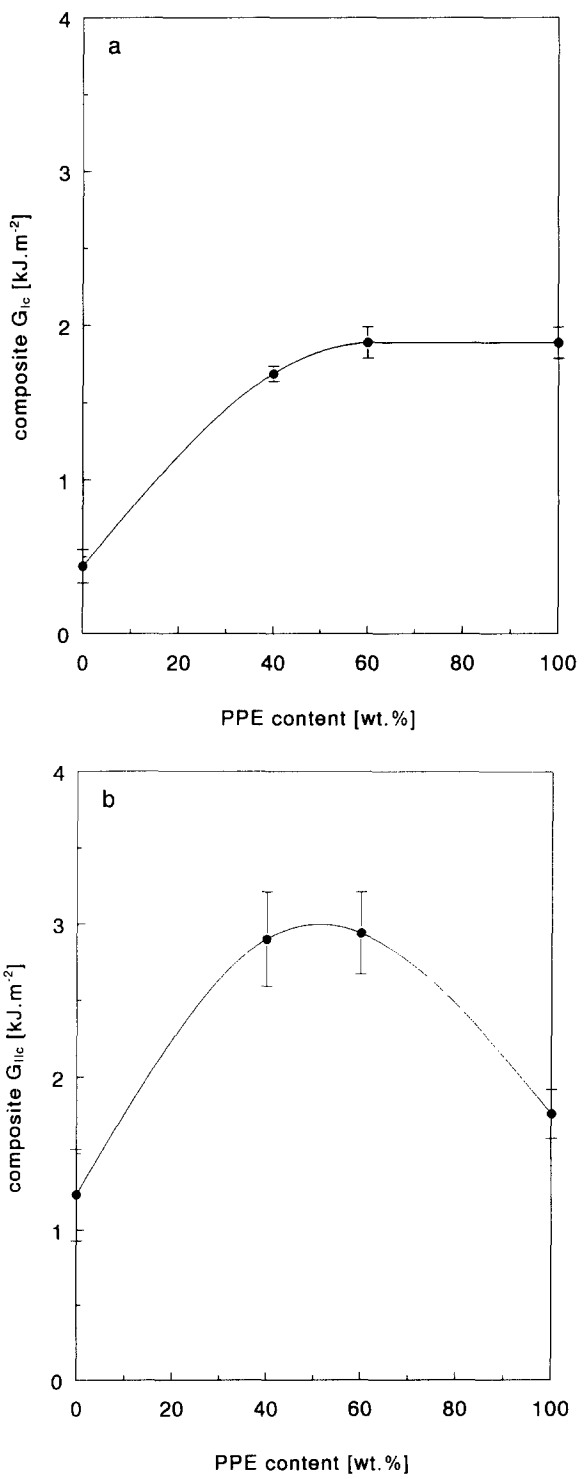

Figure 5 Critical strain energy release rate G_c of carbon fabric composites (50 vol% fibres) *versus* matrix composition: (a) mode-I; (b) mode-II

consequence is that the penalty in matrix toughness due to the use of epoxy resin as a reactive solvent is negligible and will not affect the composite performance.

In *Figure 5b* the results of the mode-II interlaminar fracture toughness experiments are presented. The results obtained in mode-II loading conditions clearly differ from those found in mode-I loading conditions, and a remarkably strong synergy in $G_{IIc}{}^{C}$ is observed for the epoxy/PPE-based laminates. In contrast to the $G_{Ic}{}^{C}$ values which are propagation values, these $G_{IIc}{}^{C}$ values are measured for crack initiation and will be lower than the propagation values. Consequently, the results do not allow for a quantitative comparison, but can be used merely to discuss the deformation behaviour of the materials qualitatively.

In order to explain the results found for the fracture toughness tests, the fracture surfaces were examined. In *Figures 6* and *7* SEM micrographs of the mode-I and mode-II fracture surfaces are presented. The micrographs clearly demonstrate the lack of adhesion in neat PPE composites, especially compared with the neat epoxy and the epoxy/PPE system. As demonstrated in *Figures 6a*

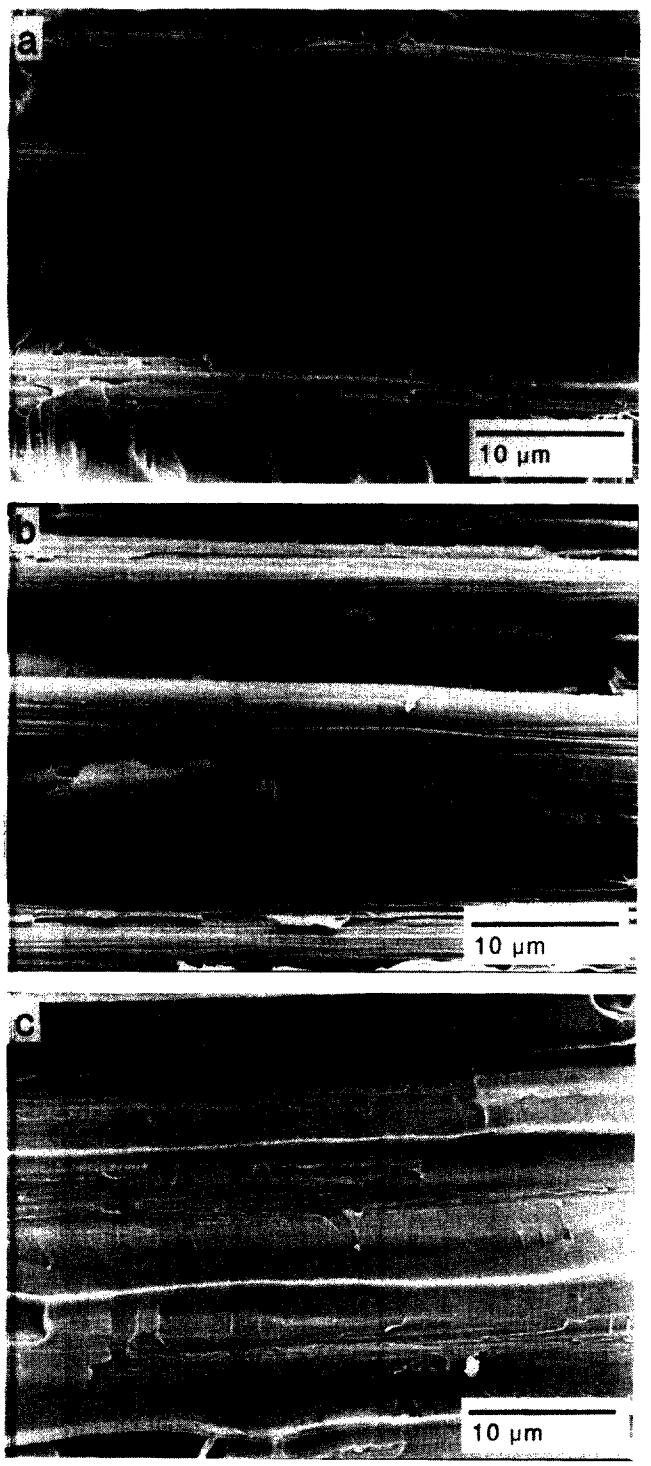

Figure 6 SEM micrographs of fracture surfaces of mode-I interlaminar fracture toughness specimens: (a) epoxy resin; (b) PPE; (c) epoxy/PPE (60 wt% PPE) matrix

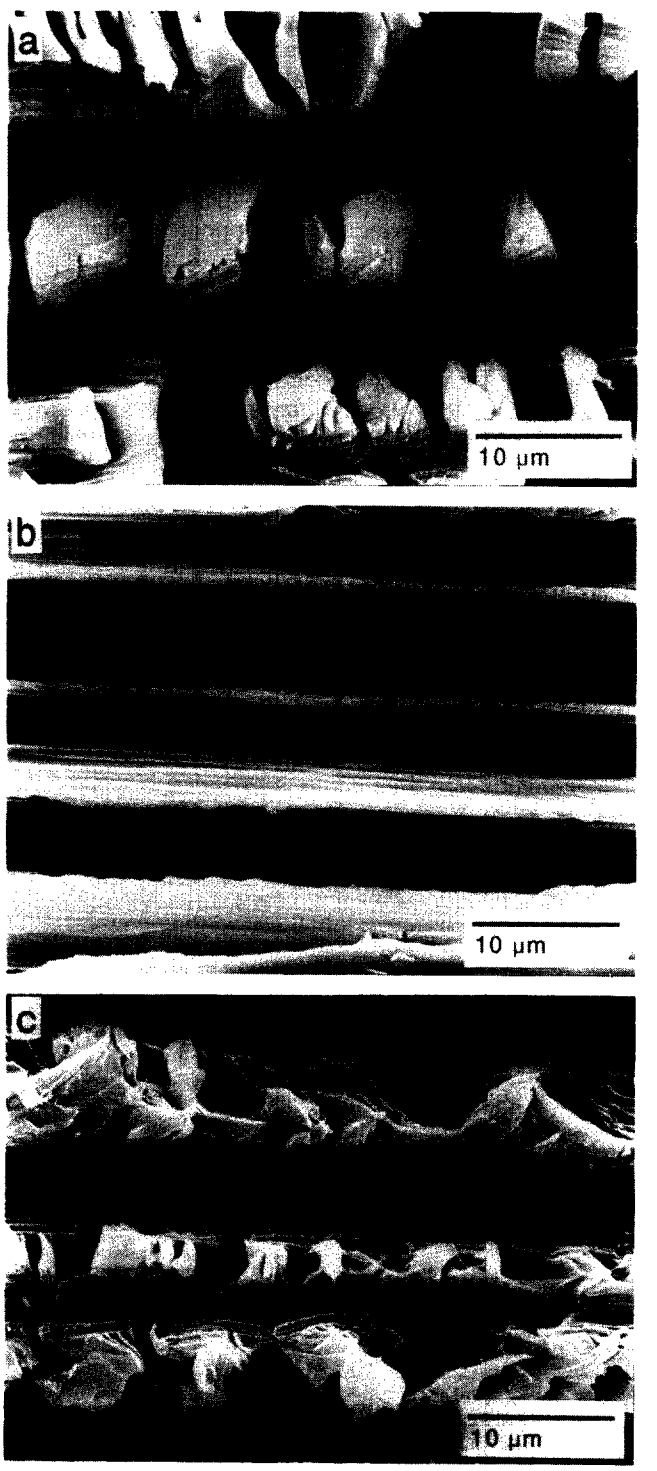

Figure 7 SEM micrographs of fracture surfaces of mode-II interlaminar fracture toughness specimens: (a) epoxy resin; (b) PPE; (c) epoxy/PPE (60 wt% PPE) matrix

and *7a*, in mode-II loading conditions the brittle epoxy resin composite reveals a significantly different crack propagation behaviour compared with mode-I loading conditions. The mode-II fracture surface shows S-shaped microcracks. This typical crack propagation behaviour, referred to in the literature as 'hackling', results in surprisingly high $G_{IIc}{}^{C}$ values for composites based on the intrinsically brittle epoxy resin. The microcracking mechanism ahead of the crack tip redistributes the load ahead of the crack tip analogous to plastic deformation and effectively increases the amount of energy absorbed ($G_{IIc}{}^{C} \approx 3G_{Ic}{}^{C}$). In contrast, for composites based on ductile matrices like PPE (*Figures 6b* and *7b*) the loading conditions do not significantly affect the deformation mode or the fracture toughness value ($G_{IIc}{}^{C} \approx G_{Ic}{}^{C}$). Both mode-I and mode-II loading conditions results in localized yielding at the crack tip and debonding due to poor interfacial adhesion. As a result, the gain in composite toughness achieved by exchanging brittle thermosets for ductile thermoplastics is generally in mode-II conditions even more disappointing than under mode-I conditions. While mode-I testing revealed a four-fold increase in toughness on exchanging epoxy resin for pure PPE, in mode-II loading conditions only a 1.5-fold increase in toughness was found.

However, for the composites based on the ductile epoxy/PPE system mode-II tests also yield markedly higher G_c values compared with mode-I tests ($G_{IIc}{}^{C} \approx 2G_{Ic}{}^{C}$). Obviously, a change in deformation mechanism has to occur similar to that observed in the pure epoxy resin system. An indication of a change in crack propagation mode with loading conditions is given in the SEM micrographs presented in *Figures 6c* and *7c*. The SEM micrograph of the mode-II specimen reveals a more extensively deformed fracture surface and a combination of yielding and brittle fracture is distinguished. The unique composite morphology may explain the observed synergy. Provided that cracks in the epoxy interlayer can initiate yielding in the PPE-rich phase, multiple brittle fracture of the epoxy interlayer during mode-II loading can effectively delocalize yielding of the PPE-rich phase ahead of the crack tip and subsequently increase the deformation volume and $G_{IIc}{}^{C}$. A schematic representation of the influence of brittle interphases on the mode-II deformation mechanism in ductile thermoplastic composites is shown in *Figure 8*.

Surprisingly, the results reveal that a brittle interphase in an intrinsically tough thermoplastic composite could act as an effective impact modifier. This observation is of particular interest, since in the existing literature attention is mainly directed towards the introduction of ductile or rubbery interphases[31–35]. In a forthcoming paper more results will be reported concerning this intriguing feature.

Impact performance

In addition to the more fundamental analyses of composite toughness via G_{Ic} and G_{IIc}, a series of simple falling weight impact experiments was conducted on the epoxy/PPE-based carbon fabric laminates. As a reference in this case only the epoxy resin composite was tested.

A pronounced difference in impact behaviour between the epoxy resin and the epoxy/PPE-based laminates was found. For neat epoxy resin penetration occurred at a low impact energy level of 9 J, while for the epoxy/PPE-based composites no penetration occurred even at high impact energy levels up to 21 J. The internal damage of the impacted specimens was studied using ultrasonic C-scan analyses. In *Figure 9* the visible damage and internal impact damage are illustrated for specimens subjected to an incident energy level of 9 J. Clearly, for the neat epoxy laminate catastrophic failure at the impact centre is observed, whereas the epoxy/PPE-based laminate reveals only a cross-shaped crack. With

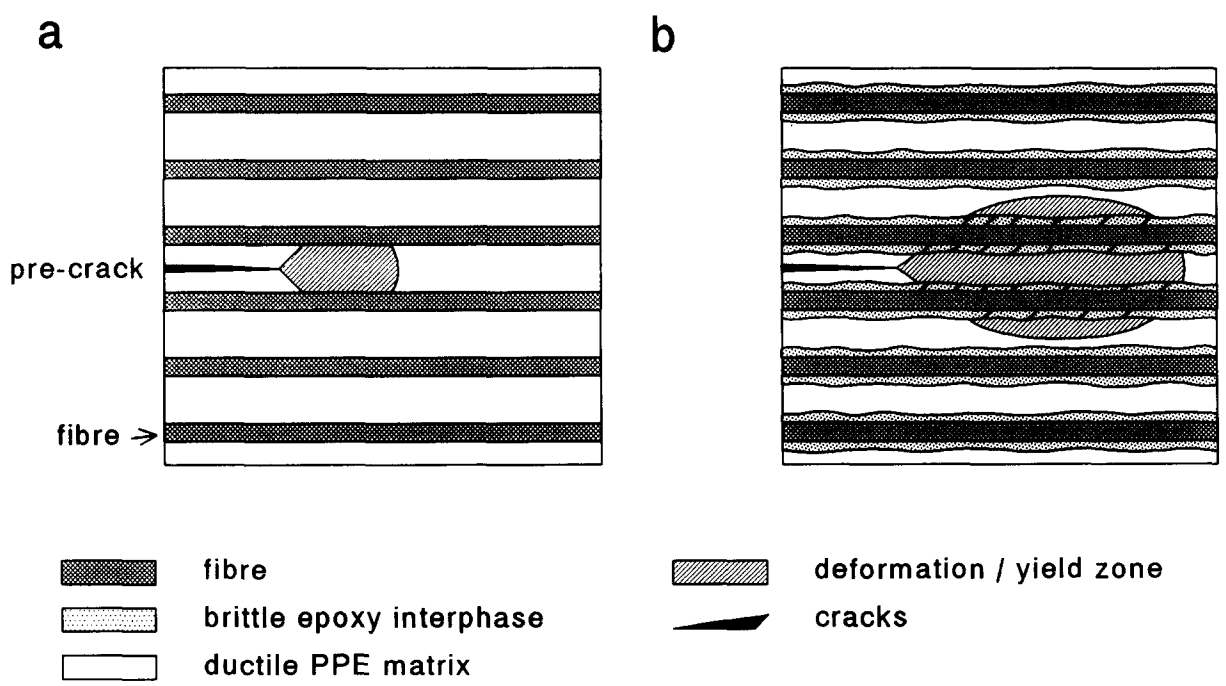

Figure 8 Schematic representation of the mode-II deformation mechanism in ductile thermoplastic composites (a) without and (b) including brittle epoxy resin interphases

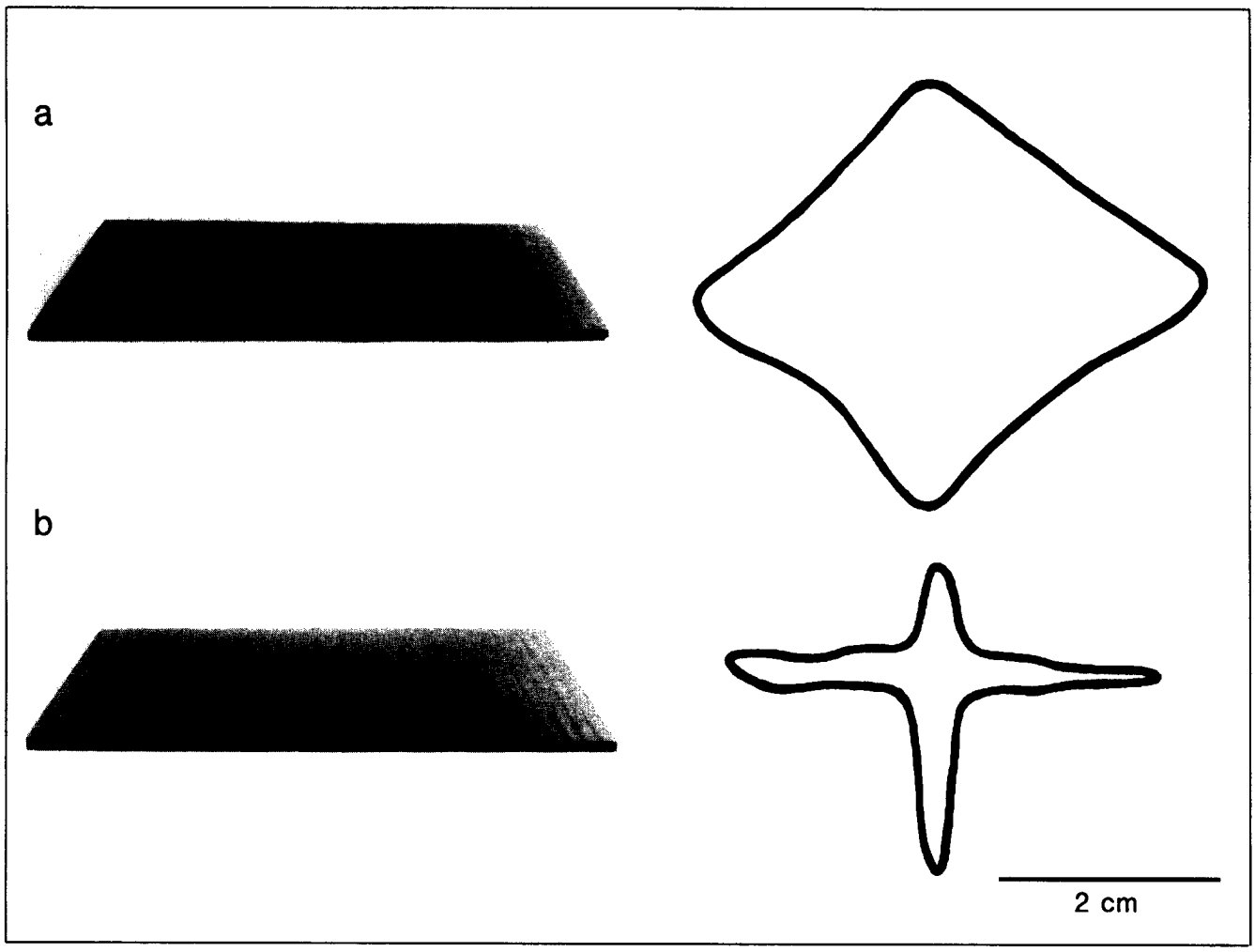

Figure 9 Tensile face damage and schematic representation of the C-scan images of carbon fabric laminates (50 vol% fibres) impacted at an energy level of 9 J: (a) epoxy matrix; (b) epoxy/PPE (60 wt% PPE) matrix

increasing impact energy this cracking or splitting process remains remarkably stable, and for high impact energies the crack proceeds to the clamps where it simply deflects. Ultrasonic C-scan analyses, depicted schematically in *Figure 9*, revealed no additional internal damage in the epoxy/PPE laminate, in contrast to the epoxy laminate where a large rectangular damage zone as a result of delamination is detected. By plotting the percentage of absorbed energy *versus* the total impact energy (see *Figure 10*), the development of damage with increasing impact energy is clearly demonstrated. In contrast to the epoxy laminates, the epoxy/PPE-based laminates absorb a constant amount of energy. This is an indication of a stable damage mechanism and is attributed to the splitting process observed. This cracking process occurs also in the neat epoxy samples, but is accompanied by delamination as a result of the low interlaminar fracture toughness. Delamination reduces the stiffness of the plate at the impact area and significantly reduces the ability to store elastic energy. Hence, for the epoxy laminates penetration occurs at a low impact energy level.

As a result of the absence of delamination in the epoxy/PPE-based laminates, in *Figure 11a* the damage is presented in terms of the maximum damage length or crack length rather than the frequently used total damage area or delaminated area. At low impact energy levels the damage observed in the epoxy/PPE system is lower compared with the damage in the epoxy laminates. However, owing to the higher penetration resistance, in the epoxy/PPE specimens eventually more damage is generated. As illustrated in *Figure 11a*, this effect is rather extreme since the maximum damage length is simply

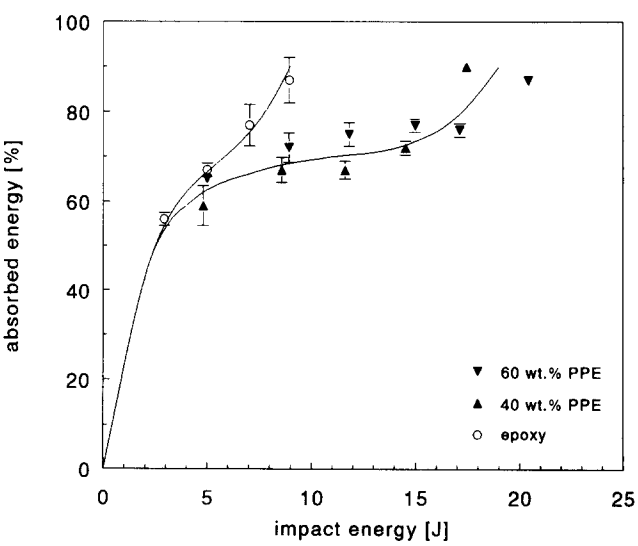

Figure 10 Percentage of impact energy absorbed *versus* total impact energy for epoxy-based and epoxy/PPE-based (40 and 60 wt% PPE) laminates (50 vol% fibres)

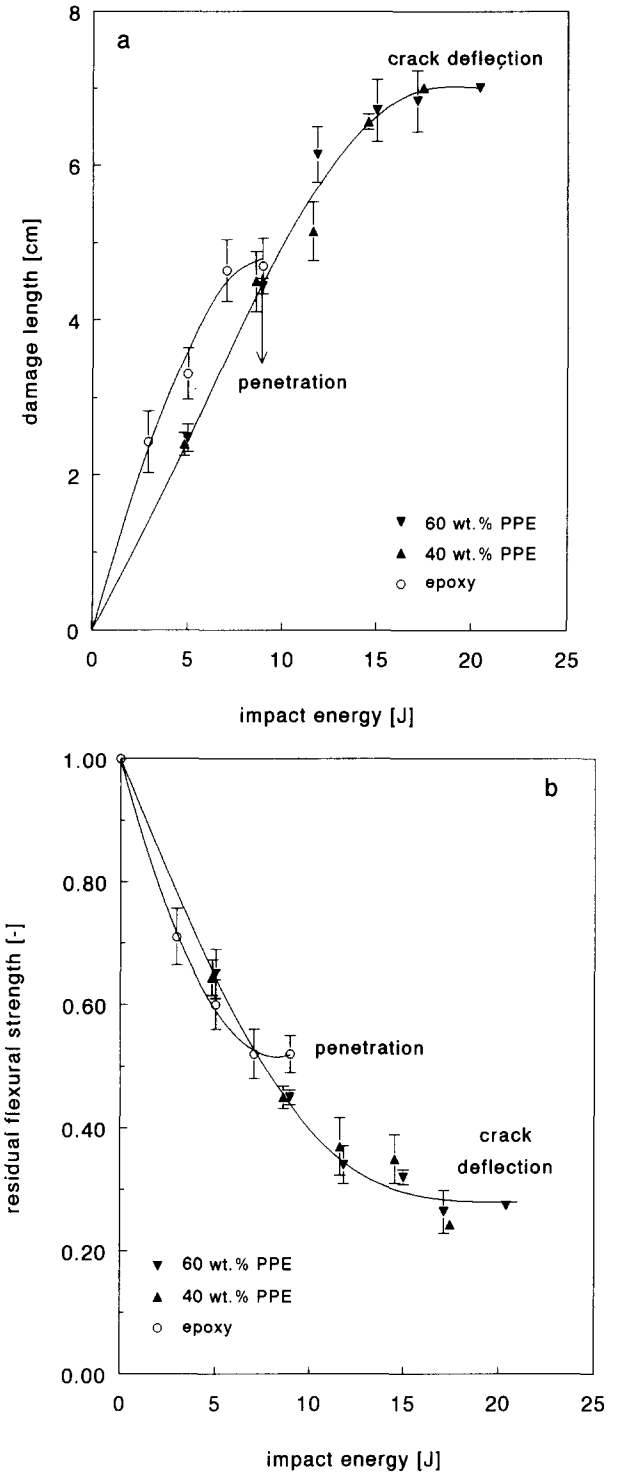

Figure 11 (a) Damage length and (b) residual flexural strength *versus* total impact energy for epoxy-based and epoxy/PPE-based (40 and 60 wt% PPE) laminates (50 vol% fibres)

determined by the clamping width (8 cm). The residual flexural strengths of the impacted samples are plotted in *Figure 11b*. Since the reduction in flexural strength is mainly governed by fibre breakage, the same trends are observed as in *Figure 11a*.

The absolute reduction in damage and the subsequent residual strength as anticipated from the results of the interlaminar fracture toughness experiments are rather small. This is the result of the type of damage generated, i.e. a fibre-dominated cracking process instead of delamination. The high toughness of the epoxy/PPE-based composites affects the damage process only indirectly by preventing delamination and yields a significant increase in penetration resistance compared with the epoxy laminates. Obviously, interlaminar toughness will only correlate with impact performance in the case of a delamination-dominated damage mechanism. For this reason, samples with a larger thickness (5 mm) and a quasi-isotropic lay-up more susceptible to delamination damage were tested. The

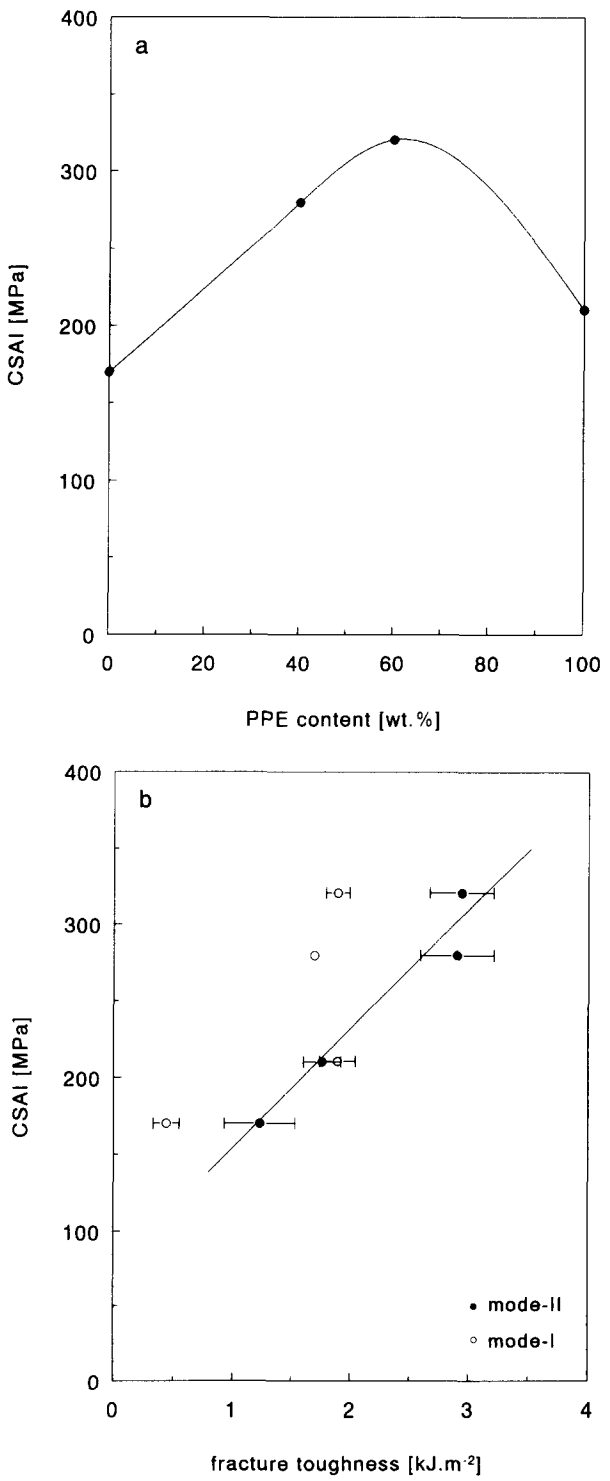

Figure 12 BOEING compressive strength after impact (6.7 J mm^{-1}) of carbon fabric reinforced composites (50 vol% fibres) *versus* (a) matrix composition and (b) mode-I and mode-II interlaminar fracture toughness

impact performance of these laminates was studied by means of the BOEING compression after impact test. In this test the impact performance is expressed in terms of the residual compressive strength (CSAI) of a composite plate subjected to a normalized impact event (6.7 J mm^{-1}).

The results of this second series of impact tests are presented in *Figure 12a*. Although the absolute values found for the carbon fabric reinforced composites are difficult to compare with values reported for quasi-isotropic composites based on unidirectional plies, the epoxy/PPE composites exhibit high CSAI values in the range of values found for tough composite materials presented in the literature[12,19,36]. Owing to the change in composite design, the epoxy/PPE specimens revealed mainly delamination damage. Consequently, in contrast to the first series of impact tests, the results found for the BOEING impact tests correlate well with the results of the interlaminar toughness tests. Clearly, again a strong synergy in properties in accordance with the mode-II fracture toughness tests is observed for the epoxy/PPE-based composites.

The results of the BOEING impact tests clearly reveal the importance of the synergy observed in mode-II fracture toughness. As shown in the literature[2,12,19,37], mode-II rather than mode-I interlaminar fracture toughness correlates with the impact performance of composite materials. This correlation can be attributed to the amount of damage generated during the impact incident, which is, although rather complex, mainly shear dominated. The importance of G_{IIc}^{C} for assessing the composite impact performance is illustrated in *Figure 12b*, revealing a linear correlation between CSAI and G_{IIc}^{C}.

An interesting feature inherent to the impregnation route presented in this paper is that the mechanical properties of the *in situ* generated fibre/matrix interphase can be tuned through variations in the type of epoxy resin solvent used. Our present research is aimed at new solvent systems that yield a broad range of mechanical properties of the interphase. This provides a powerful technique to study the correlation between interphase characteristics and the macroscopic composite performance. For instance, increasing the ductility of the epoxy interphase is an elegant way of evaluating the toughening mechanism, as proposed in this paper. The results of this investigation will be reported in a forthcoming paper.

CONCLUSIONS

The use of epoxy resin as a reactive solvent facilitates the introduction of PPE into high quality thermoplastic composite structures using a simple film-stacking technique. Upon curing, phase separation is initiated and the epoxy resin is converted into a second phase. As a result of the polarity of the fibres present, the epoxy resin preferentially accumulates at the fibre surface, resulting in an epoxy interlayer or interphase at the fibres. Consequently, the epoxy resin is not only effective as a solvent, enabling processing of PPE and facilitating impregnation, but also forms a structural part of the final composite material. The epoxy interphase provides a high level of interfacial adhesion which is not attainable in the pure PPE system. At a high fibre volume fraction, a morphology of epoxy-coated fibres in a virtually pure PPE matrix is obtained. As a result of this unique morphology, the composite materials reveal outstanding properties in terms of interlaminar toughness and impact performance. The results indicate that apart from the major advantage of a high level of interfacial adhesion, multiple brittle fracture of the epoxy interphase during mode-II loading (impact) can effectively delocalize damage. This could be a new toughening mechanism for thermoplastic composite materials.

ACKNOWLEDGEMENTS

This research was financially supported by General Electric Plastics (Bergen op Zoom, The Netherlands). The authors thank Professor J. Bussink for many stimulating discussions and J. G. L. Nelissen for assistance in the experiments. The Catholic University of Leuven (Belgium) and, in particular, V. Efstratiou are acknowledged for their assistance in the impact tests.

REFERENCES

1 Sela, N. and Ishai, O. *Composites* 1989, **20**, 423
2 Cantwell, W. J. and Morton, J. *Composites* 1991, **22**, 347
3 Carlsson, L. A. (Ed.) 'Thermoplastic Composite Materials', Composite Materials Series, Vol. 7, Elsevier, Amsterdam, 1991
4 Cogswell, F. N. 'Thermoplastic Aromatic Polymer Composites', Butterworth-Heinemann, Oxford, 1992
5 Bussink, J., Sederel, W. L. and Minderhout, W. 'Kunststoff-Handbuch, Band 3/2: Technische Thermoplaste', Hanser, Munich, 1993
6 Wu, G. M., Schultz, J. M., Hodge, D. J. and Cogswell, F. N. in 'Proceedings of the 48th Annual Technical Conference of the Society of Plastics Engineers', Society of Plastic Engineers, Brookfield Center, 1990, p. 1390
7 Venderbosch, R. W., Meijer, H. E. H. and Lemstra, P. J. *Polymer* 1994, **35**, 4349
8 Bucknall, C. B. and Partridge, I. K. *Polymer* 1983, **24**, 639
9 Kim, S. C. and Brown, H. R. *J. Mater. Sci.* 1987, **22**, 2589
10 Wang, Z., Chen, D. and Liu, X. *J. Adhes.* 1987, **23**, 201
11 Muraki, T., Takeo, A. and Hirata, M. in 'Materials Science Monographs' (Eds K. Brunsch, H. D. Gölden and C. M. Herkert), Vol. 35, Elsevier, Amsterdam, 1986, p. 163
12 Odagiri, N., Muraki, T. and Tobukuro, K. in 'Science of Advanced Materials and Process Engineering Series (Eds G. Carrilo, E. D. Newell, W. D. Brown and P. Phelan), Vol. 33, Society for the Advancement of Material and Process Engineering, Covina, 1988, p. 272
13 Sefton, M. S., McGrail, P. T., Peacock, J. A., Wilkinson, S. P., Crick, R. A., Davies, M. and Almen, G. in 'International SAMPE Technical Conference Series' (Eds T. Lynch, J. Perch, T. Wolf and N. Rupert), Vol. 19, Society for the Advancement of Materials and Process Engineering, Covina, 1987, p. 700
14 Almen, G. R., MacKenzie, P., Malhotra, V., Maskell, R. K., McGrail, P. T. and Sefton, M. S. in 'International SAMPE Technical Conference Series' (Eds H. L. Chess, S. P. Prosen, J. W. Davis and J. A. Heth), Vol. 20, Society for the Advancement of Materials and Process Engineering, Covina, 1988, p. 46
15 Bucknall, C. B. and Gilbert, A. H. *Polymer* 1989, **30**, 213
16 Yamanaka, K. and Inoue, T. *Polymer* 1989, **30**, 662
17 Bauer, R. S., Stenzenberger, H. D. and Römer, W. in 'Science of Advanced Materials and Process Engineering Series' (Eds G. A. Zakrzewski, D. Marenko, S. T. Peters and C. D. Dean), Vol. 34, Society for the Advancement of Materials and Process Engineering, Covina,1989, p. 899
18 Bauer, R. S., Stenzenberger, H. D. and Römer, W. in 'Science of Advanced Materials and Process Engineering Series', Vol. 35, Society for the Advancement of Materials and Process Engineering, Covina,1990, p. 395
19 Recker, H. G., Altstädt, V., Eberle, W., Folda, T., Gerth, D., Heckmann, W., Ittemann, P., Tesche, H. and Weber, T. *SAMPE J.* 1990, **26**, 73
20 Hourston, D. J., Lane, J. M. and MacBeath, N. A. *Polym. Int.* 1991, **26**, 17
21 Hedrick, J. L., Yilgor, I., Jurek, M., Hedrick, J. C., Wilkes, G. L. and McGrath, J. E. *Polymer* 1991, **32**, 2020

22 MacKinnon, A. J., Jenkins, S. D., MacGrail, P. T. and Pethrick, R. A. *Macromolecules* 1992, **25**, 3492
23 MacKinnon, A. J., Jenkins, S. D., McGrail, P. T. and Pethrick, R. A. *Polymer* 1993, **34**, 3252
24 Pearson, R. A. and Yee, A. F. *J. Appl. Polym. Sci.* 1993, **48**, 1051
25 Williams, J. G. and Cawood, M. J. *Polym. Test.* 1990, **9**, 15
26 Davies, P. 'Protocols for Interlaminar Fracture Testing of Composites', Report of the European Structural Integrity Society, Polymers and Composites Task Group, Ecole Polytechnique Federale de Lausanne, Switzerland, 1992
27 Drzal, L. T., Waterbury, M. C. and Madhukar, M. in 'Science of Advanced Materials and Process Engineering Series' (Eds G. C. Grimes, R. Turpin, G. Forsberg, B. M. Rasmussen and J. Whitney), Vol. 37, Society for the Advancement of Materials and Process Engineering, Covina,1992, p. 770
28 Hughes, J. D. H. *Compos. Sci. Technol.* 1991, **41**, 13
29 Jones, C. *Compos. Sci. Technol.* 1991, **42**, 275
30 Bradley, W. L. in 'Application of Fracture Mechanics to Composite Materials' (Ed. K. Friedrich), Composite Materials Series, Vol. 6, Elsevier, Amsterdam, 1989, p. 159
31 Kim, J. and Mai, Y. *Compos. Sci. Technol.* 1991, **41**, 333
32 Schwartz, H. S. and Hartness, J. T. in 'Toughened Composites' (Ed. N. Johnston), ASTM STP 937, American Society for Testing and Materials, Philadelphia, PA, 1987, p. 150
33 Piggott, M. R. *Mater. Res. Soc. Symp. Proc.* 1989, **170**, 265
34 Gerard, J. F. *Polym. Eng. Sci.* 1988, **28**, 568
35 McGarry, F. J. *Adv. Chem. Ser.* 1989, **222**, 175
36 Evans, R. E. and Masters, J. E. in 'Toughened Composites' (Ed. N. Johnston), ASTM STP 937, American Society for Testing and Materials, Philadelphia, PA, 1987, p. 413
37 Prichard, J. C. and Hogg, P. J. *Composites* 1990, **21**, 503